Strategies towards controlling strain-induced mesoscopic phase separation in manganite thin films

2008 J. Phys.: Condens. Matter 20 434228

(http://iopscience.iop.org/0953-8984/20/43/434228)

IOP PUBLISHING JOURNAL OF PHYSICS: CONDENSED MATTER

J. Phys.: Condens. Matter **20** (2008) 434228 (8pp) doi:10.1088/0953-8984/20/43/434228

Strategies towards controlling strain-induced mesoscopic phase separation in manganite thin films

H-U Habermeier

Max-Planck-Institut für Festkörperforschung, Heisenbergstrasse 1, D 70569 Stuttgart, Germany

Received 7 July 2008
Published 9 October 2008
Online at stacks.iop.org/JPhysCM/20/434228

Abstract

Complex oxides represent a class of materials with a plethora of fascinating intrinsic physical functionalities. The intriguing interplay of charge, spin and orbital ordering in these systems superimposed by lattice effects opens a scientifically rewarding playground for both fundamental as well as application oriented research. The existence of nanoscale electronic phase separation in correlated complex oxides is one of the areas in this field whose impact on the current understanding of their physics and potential applications is not yet clear. In this paper this issue is treated from the point of view of complex oxide thin film technology. Commenting on aspects of complex oxide thin film growth gives an insight into the complexity of a reliable thin film technology for these materials. Exploring fundamentals of interfacial strain generation and strain accommodation paves the way to intentionally manipulate thin film properties. Furthermore, examples are given for an extrinsic continuous tuning of intrinsic electronic inhomogeneities in perovskite-type complex oxide thin films.

(Some figures in this article are in colour only in the electronic version)

1. Introduction

The simultaneous occurrence of phases with different electronic ground states separated at mesoscopic or nanoscopic length scales in otherwise chemically homogeneous complex oxide systems and their mutual interaction is a research area of growing interest in both fundamental science and application oriented technology [1]. Generally, there are two different concepts of phase separation, the artificial phase separation in thin film heterostructures and superlattices, and the intrinsic phase separation in oxide compounds with strong electron–electron interaction in a certain composition and temperature range. The latter seems to be a general feature for correlated oxide compounds in which cations surrounded by oxygen octahedra can occur in mixed valence states, and a delicate interplay of spin, charge, orbital and lattice interactions takes place. The activities covering the former are aimed at exploring the potential mutual electronic interactions of correlated oxide compounds in analogy to artificially tailored semiconductor as well as metal heterostructures and superlattices (SLs). Artificially tailored semiconductor heterostructures, for example, are demonstrated to generate high-mobility electron systems with tunable densities at their interface and have proven to form the basis for unexpected advances in science and device technology over the past decades [2]. Similarly, metal superlattices consisting of ferromagnetic and nonmagnetic layers form the basis of devices exhibiting a giant magnetoresistance and are key elements in modern information technology [3]. The attempt to replicate such multilayers using transition metal oxides paves the way for an even more exciting research area due to the rich intrinsic phase behavior of the transition metal oxides arising from the interplay of spin, charge, lattice and orbital ordering. The reason for this plethora of interactions comes from the electrons occupying the 3d shell of transition metals whose degeneracy is lifted by the crystal field of the surrounding oxygen. The occupancy of 3d electrons in different energy and orbital states is sensitively affected by small perturbations either by external electrical or magnetic fields or by strain fields of either intrinsic (chemical pressure, epitaxial strain in thin films) or extrinsic (hydrostatic pressure) origin. In figures 1(a) and (b), the perovskite unit cell and the corresponding electronic structure of the Mn 3d electrons are given, indicating the crystal field splitting and the lifting of degeneracy by the Jahn–Teller effect, thus causing

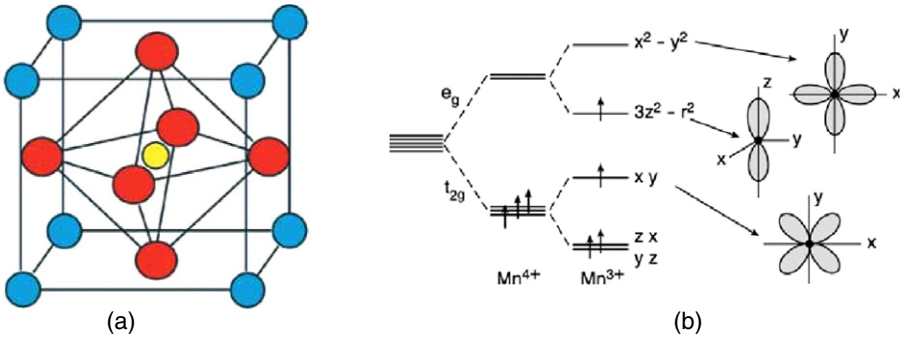

Figure 1. (a) Perovskite structure of an ABO_3 compound such as $LaMnO_3$ (Mn: yellow (bright central atom), O: red (dark) and La: blue (grey)). (b) Single ion scheme of 3d electronic states in Mn^{3+} and Mn^{4+} ions in perovskite manganites.

a nominally 100% spin polarization of the electrons in the e_g band and a strong coupling of the electronic system to the lattice.

In contrast to elemental semiconductors and semiconductor III–V compounds, where the constituents show basically all one valence state—independent of doping—the main characteristics of the transition metals in correlated oxide compounds is their stability in different and even in mixed valence states. Combining such transition metal oxides in heterostructures or superlattices can give rise to novel quantum states at the interfaces with properties and functionalities qualitatively beyond those attainable in semiconductors. In the past few years this field has attracted increasing interest in the science community and is listed amongst the 'runners-up' in the breakthrough of the year 2007 category in *Science* magazine [4–7].

For investigations of the concept of intrinsic phase separation superconducting cuprates and the manganite systems serve as prototype materials. The richness in magnetic ordering in manganites and the search for the coupling mechanism giving rise to superconductivity in cuprates are the driving forces to explore the relation of intrinsic inhomogeneities and physical properties in these materials.

Investigations of perovskite-type hole-doped rare earth manganites with the chemical formula $RE_{1-x}AE_xMnO_3$ (RE is a trivalent rare earth ion and AE a divalent alkaline earth ion) revealed various novel properties caused by a complex interplay of spin, charge, lattice and orbital ordering. As the focus of interest are the metal–insulator transition at the Curie temperature, T_C, the phenomenon of charge ordering and the colossal magnetoresistance (CMR) effect. Furthermore, the manganites can serve as a prototype material for basic studies of strong electron correlation and electron–lattice coupling effects and, due to the high degree of spin polarization, they represent an excellent candidate for potential spintronics device applications. One of the most important recent discoveries in correlated oxide compounds is the coexistence and/or competition of several phases at the nanoscale level, commonly described as mesoscopic phase separation [1]. This nanoscale phase separation has been predicted theoretically and has been proven experimentally in several material systems such as cuprates, vanadates and titanates [1]. It appears to be a general feature of compounds with strong electron correlations in which cations surrounded by oxygen octahedra occur in a valence state where Jahn–Teller distortions are present and consequently a strong coupling of the lattice with the electronic system is taking place. Electronic phase separation is increasingly regarded as a phenomenon of importance to understand the magnetic and transport properties of transition metal oxides with strong electron correlation. In doped rare earth manganites a rich variety of different phases can exist or coexist which exhibit ferromagnetism, antiferromagnetism, metallicity and charge ordering, depending on their composition, size of A-site cations and external factors such as magnetic or electrical fields. The coexistence and/or competition of phases are a consequence of the complexity of electronic and electron–lattice interactions at comparable energy scales.

This paper deals with the formation of epitaxial strain and strain relaxation in manganite thin films and the possibility to externally manipulate mesoscopic phase separation in them as a case study for the more general treatment of external manipulation of the phase separation in perovskite-type complex oxide thin films. In section 2 relevant aspects of perovskite thin film deposition technology is outlined, section 3 covers epitaxial strain evolution and strain relaxation in manganites and in section 4 an outlook is given for the possibilities of extrinsic continuous modification of electronic inhomogeneities in perovskite thin films.

2. Comments on perovskite thin film growth

2.1. General aspects

The key requirement for an investigation of intrinsic phase separation problems in perovskite thin films is the availability of a mature technology suitable to deposit single-crystal-type films with a structural and compositional homogeneity at a length scale given by the short interaction lengths for the cooperative phenomena such as superconductivity and ferromagnetism, which are typically of the order of 1 nm. The difficulties in achieving such perfect complex oxide thin films (COTFs) are not only caused by the necessity to have the correct particle flux ratio of the constituents at the substrate site, forming the correct crystal structure, but also by the complex parameter space for the deposition

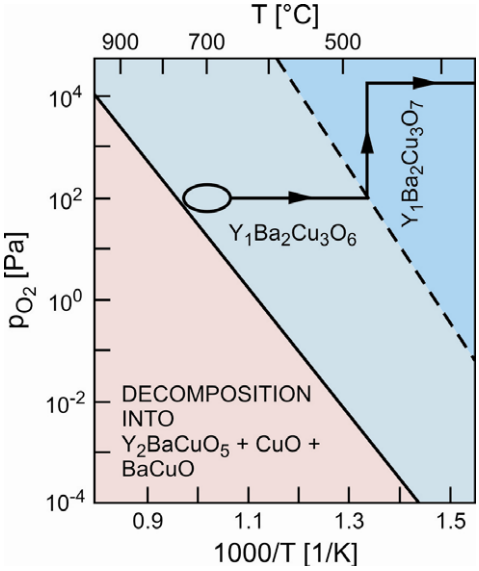

Figure 2. Phase stability diagram p_{O_2}/T for $YBa_2Cu_3O_7$ thin film deposition.

of films with the desired crystallographic orientation and oxygenation state. This includes the deposition rate, kinetic energy of the particles impinging the substrate surface, substrate flatness and termination, and the thermodynamic requirements for phase stability as well. As an example the oxygen pressure/temperature phase stability diagram for $YBa_2Cu_3O_{7-x}$ (YBCO) is given in figure 2 [8] with the phase stability line for the Cu^+/Cu^{2+} decomposition and the conversion line of the tetragonal non-superconducting phase to the orthorhombic superconducting one by oxygen incorporation (broken line). The black line with the arrows indicates the conventional path to obtain high quality fully oxygenated films with high critical temperature and high critical current.

Within the parameter range set by the phase stability criteria, thermodynamic and kinetic factors determine the growth. The nucleation and growth mode is governed by the relative supersaturation, μ determining the chemical potential, σ as the driving force for the film growth. They are related by

$$\sigma = k_B T_s \ln \mu = k_B T_s \ln(\Phi \Delta T / R T_s^2), \quad (1)$$

where k_B is the Boltzmann constant, Φ denotes the molar heat of solution, ΔT the undercooling, and R and T_s are the gas constant and the absolute temperature of the substrate. Depending on the supersaturation either dislocation-controlled spiral growth (small supersaturation) or two-dimensional nucleation (island formation) occurs up to a critical supersaturation μ^*. Further increase of μ causes a transition to unstable growth. Uncontrolled nucleation of growth centers on top of each other leads to a dendritic growth type [9]. In addition to supersaturation the deposition temperature, T_s, plays an important role in determining the growth kinetics and the surface morphology of the films. The relevant quantity is the normalized bonding energy, $E_b^{(i)}$, for the different species, i:

$$E_b^{(i)} = 4\Phi_{ss}^{(i)}/2k_B T_s \quad (2)$$

($\Phi_{ss}^{(i)}$ denote the potential energy of a solid–solid nearest-neighbor pair of atoms in the substrate unit cell). It is obvious that increasing deposition temperature implies a smaller E_b, causing a higher density of kink sites on the substrate surface and a more rapid growth. For the spontaneous nucleation of a unit cell a critical volume of the deposited material is required. Since single atoms are impinging the substrate, diffusion is required to ensure that a nucleus has the appropriate constituents to grow. The diffusion coefficients for the different cations, however, can differ drastically; for YBCO e.g. they vary by four orders of magnitude from Y (10^{-13} $m^2\,s^{-1}$) to Cu (10^{-9} $m^2\,s^{-1}$) at a deposition temperature, T_s, of 800 °C. Consequently, the probability for the formation of nanoprecipitates and compositional phase separation is facilitated [10, 11] if the process is not tuned precisely. The deposition parameters sensitively affect the growth behavior of complex oxide thin films and thus their defect structure and intrinsic strain state. Any generalized conclusions concerning macroscopic film properties and electronic mesoscopic phase separation in thin films have to take into account these rather elementary—albeit frequently neglected—facts. In a very systematic way Naito *et al* have investigated the simplest case, i.e. the homoepitaxial growth of $SrTiO_3$ (STO) thin films on STO(001)-oriented substrates by reflection high energy electron diffraction (RHEED) and atomic force microscopy (AFM) in order to improve the understanding of the basic processes in the epitaxial growth of perovskite thin films [12]. They could demonstrate that, under certain growth conditions, the homoepitaxial growth of $SrTiO_3$ essentially proceeds in the layer-by-layer 2D nucleation and growth with the basic unit of one unit cell. This cyclic process due to unit-cell-by-unit-cell growth is confirmed by undamped RHEED oscillations and the corresponding temporal evolution of AFM images of the growth front. By changing growth temperature or oxidation condition, crossovers from layer-by-layer growth to step-flow-like growth and from layer-by-layer growth to 3D island growth through Stranski–Krastanov growth are observed with inherent implications on the microscopic defect structure of films.

2.2. Substrate requirements

For the development of a reliable deposition technology suitable to investigate the intrinsic properties of COTFs, the choice of the substrate material is of primary importance. The optimal substrate has to meet the conditions of (i) crystallographic lattice match between film and substrate to avoid strain-induced defect generation, (ii) similar thermal expansion coefficients of film and substrate, (iii) no chemical interaction at the interface between film and substrate, and (iv) suitably terminated surfaces, structurally as well as chemically stable. In general, it is nearly impossible to find substrates fulfilling all these requirements simultaneously. Typical candidates are $LaAlO_3$, $SrTiO_3$ and MgO for cuprate and manganite thin film deposition. In table 1 some of the most frequently used substrates and their properties are listed. Substrates, however, are much more than merely a chemically inert mechanical support for thin films; they are functional

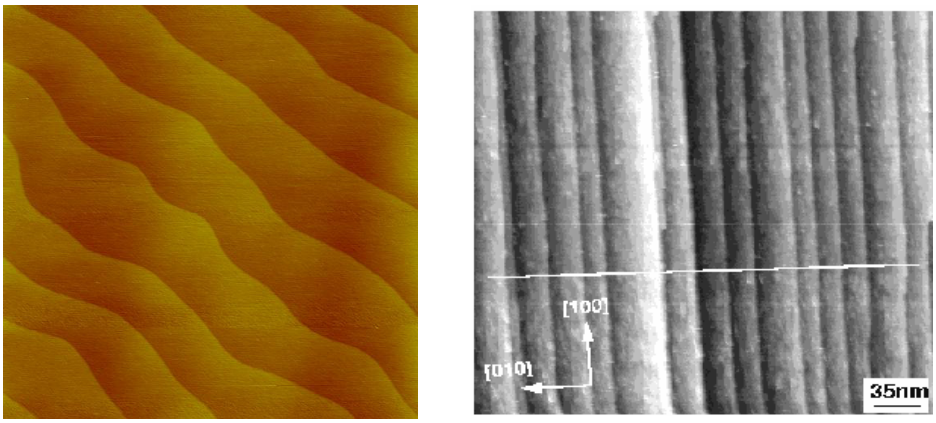

Figure 3. (a) TiO_2 terminated $SrTiO_3$ surface (5 μm × 5 μm) showing large atomically flat terraces [18]. (b) Step and terrace structure of a $SrTiO_3$ surface with a vicinal cut of 1.2° versus [010] taken from [16].

Table 1. Properties of substrates suitable for complex oxide thin film deposition.

Substrate materials	Thermal expansion coefficient (10^{-6} °C^{-1})	Melting temperature (°C)	Available substrate size (mm diameter)	Misfit to YBCO (%)	Twinning	Chemical stability
$SrTiO_3$	9.4	2080	50	1.4	No	Good
YSZ	11.4	2550	100	6	No	Good
MgO	14	2825	>30	9	No	Poor
α-Al_2O_3	9.4	2050	100	6–11	No	Good
$LaAlO_3$	10–13	2100	100	2	Yes	Good
$LaSrGaO_4$	10	1520	15	0.26	No	Good
$LaSrAlO_4$	7.55	1650	10	2.7	No	Good
$LaGaO_3$	9	1715	40	2	Yes	Good
$NdGaO_3$	9–11	1670	50	0.04	No	Good
$PrGaO_3$	7–8	1680	10	0.3	Yes	Good

elements in thin film technology [13]. On the one side, they can be prepared as chemically well-terminated atomically flat surfaces at microscopic dimensions [14, 15]; on the other side, intentional surface miscut and subsequent recrystallization (vicinal cut substrates) enables a nanoscale tailoring of step and terrace structures of the surface [16]. Figure 3(a) represents a TiO_2 terminated STO(001) substrate with large-area atomically flat terraces interrupted by one unit cell high steps, while figure 3(b) shows the rather regular step-terrace structure of a STO(001) substrate with an intentional miscut of 1.2° towards the [010] direction. The growth mechanism of films using such substrates usually changes from the Stranski–Krastanov mode to the step-flow mode generating antiphase boundaries at the step edges if there is a mismatch of substrate and film unit cell height [16]. In the case of YBCO this causes anisotropic flux-line pinning [16], but in the case of manganites a uniaxial anisotropy of the magnetic domains [17].

2.3. Deposition techniques

Nearly all commonly used thin film deposition techniques have been more or less successfully employed for COTF and multilayer fabrication, e.g. thermal and e-beam evaporation or co-evaporation, thermal or laser molecular beam epitaxy (MBE), on-axis and off-axis high-pressure sputtering, or on-axis and off-axis pulsed laser deposition. While the *in situ* deposition route is routinely used for most of the complex oxides, the *ex situ* routes (deposition of a precursor with subsequent treatment outside of the growth chamber) are applied, if one component forms volatile oxides at deposition conditions such as the Bi- and Tl-cuprates or Na_xCoO_2. *In situ* deposition techniques usually also apply two steps, i.e. the deposition at high temperature (substrate temperature and oxygen partial pressure during deposition determined by the phase stability diagram) followed by a post-deposition oxygen treatment for the desired oxygenation. A comparative overview addressing the common features and the differences of the deposition techniques is given in a recent review paper [18].

3. Interfaces and epitaxial strain in manganite thin films

3.1. General remarks

Strictly speaking, an interface is a two-dimensional region between two three-dimensional objects. From the crystallographic point of view an interface can be either coherent (the plane of the discontinuity is a common element of both lattices) or incoherent. In this case, the interface has an amorphous character and is considered as a region of structural adjustment.

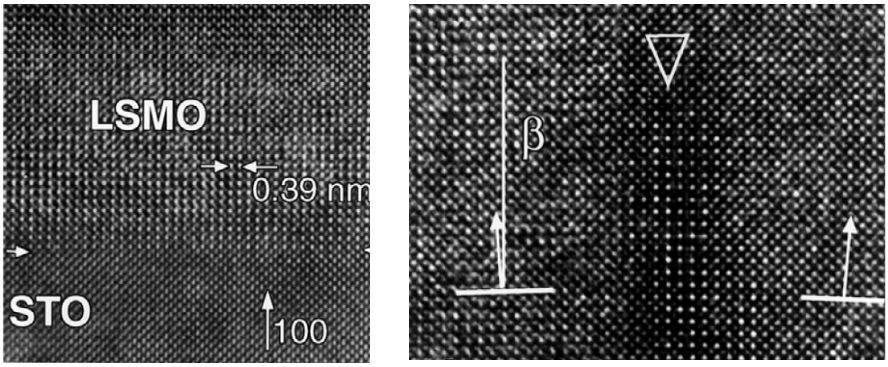

Figure 4. (a) High-resolution cross-sectional TEM image of a homogeneously strained 9 nm thick $La_{0.9}Sr_{0.1}MnO_3$ film on STO [21]. (b) High-resolution cross-sectional TEM image of a part of a 100 nm thick $La_{0.9}Sr_{0.1}MnO_3$ film on STO showing microtwinning [21].

Well-defined and nearly perfect single-crystal surfaces of oxide perovskites are a prerequisite to deposit single-crystal-type COTFs. In the ideal case, they are atomically flat, perfectly lattice matched, chemically stable and have the same thermal expansion coefficients as the thin film material. Any deviations from this ideal configuration lead to strained films and/or defect generation. This misfit can induce different types of perovskite distortions depending on the type of stress (compressive or tensile). One key issue of heteroepitaxy is that the strain, induced by the lattice mismatch, always finds a possibility to relax as the film thickness is increased. In addition to the general mechanisms such as roughening, introduction of misfit dislocations or stacking faults, COTFs can accommodate strain by distortions of the oxygen octahedra surrounding the cations and/or modifications of the oxygen stoichiometry. Epitaxial strain $\varepsilon = (a_S - a_F)/a_S$—where a_S and a_F denote the lattice parameters of substrate and film, respectively—will cause the generation of misfit dislocations (strain energy > dislocation formation energy) for a certain thickness. Thermal strain due to the difference in the thermal expansion coefficient of film and substrate or film A/film B additionally affects the film cohesion and can generate crack formation and even partial delamination. For simplicity, misfit generation and accommodation in manganite thin films of the $RE_{1-x}AE_xMnO_3$ type are treated in the following. The results, however, can be generalized to a great extent for all perovskite-based thin film materials.

3.2. Small misfit ($a_F \sim a_S$)

In the case of small misfit between substrate and film ($\Delta a/a < 1\%$) epitaxial strain is accommodated purely elastically for very thin films; in thicker films (thickness $t = 20$–100 nm) a structure consisting of periodic microtwins is formed. Using $La_{0.9}Sr_{0.1}MnO_3$ (LSMO) films deposited on STO (100)-oriented substrates, transmission electron microscopy (TEM) studies can consistently be interpreted on the assumption that misfit stresses influence the structure and microstructure of the films [19]. LSMO films of this composition are particularly suited to demonstrate this effect due to their vicinity to a phase boundary between the rhombohedric and orthorhombic structures. The macroscopic properties of such films such as resistivity and magnetization depend strongly on film thickness, i.e. the stress state of the film [20]. Depending on film thickness they are either insulating like the bulk material ($t > 50$ nm) or ferromagnetic and metallic for $t < 20$ nm with a thickness-dependent metal–insulator transition of ∼230 K. The rhombohedric and orthorhombic structures are topologically similar, but differ in features that are sensitive to applied stress, such as the tilt axis and tilt angle of the oxygen octahedra. In all cases the film–substrate interface is completely coherent, i.e. free of misfit dislocations.

In figures 4(a) and (b) the high-resolution cross-sectional TEM images of a 9 nm and a 100 nm $La_{0.9}Sr_{0.1}MnO_3$ film deposited on an STO (100)-oriented substrate is given, showing a section of the homogeneously strained thin film (figure 4(a)) and a microtwinned one (figure 4(b)). Different film thicknesses lead to different rhombohedral deformation. Thin films (9 nm) are rhombohedral without any planar defects (figure 4(a)); thicker films (100 nm) have also a rhombohedral structure but are microtwinned. The width of the twins are around 50–60 nm, close to the periodic separation for dislocations at the critical thickness for LSMO. In addition to TEM investigations systematic x-ray studies of the strain relaxation behavior of LSMO films on STO film thicknesses varying from 12 to 110 nm showed that the strained films exhibit an intriguing strain accommodation scenario: they first develop periodic one-dimensional (1D) twinning modulation waves which progressively develop into a twin domain (TD) pattern as the film thickness increases [21].

In the case of small lattice mismatch periodic microtwinning is found to be a novel mechanism to accommodate misfit strain in epitaxial growth.

3.3. Large misfit ($\Delta a/a > 1\%$)

$La_{0.7}Ca_{0.3}MnO_3$ (LCMO) is a ferromagnetic metal below the Curie temperature of 275 K and its structure is most commonly described as a cubic or a tetragonally distorted perovskite. The x-ray diffractogram of LCMO thin films can roughly be indexed on the basis of a cubic lattice with a lattice parameter $a_p = 0.384$ nm, which is compatible with a perovskite-type

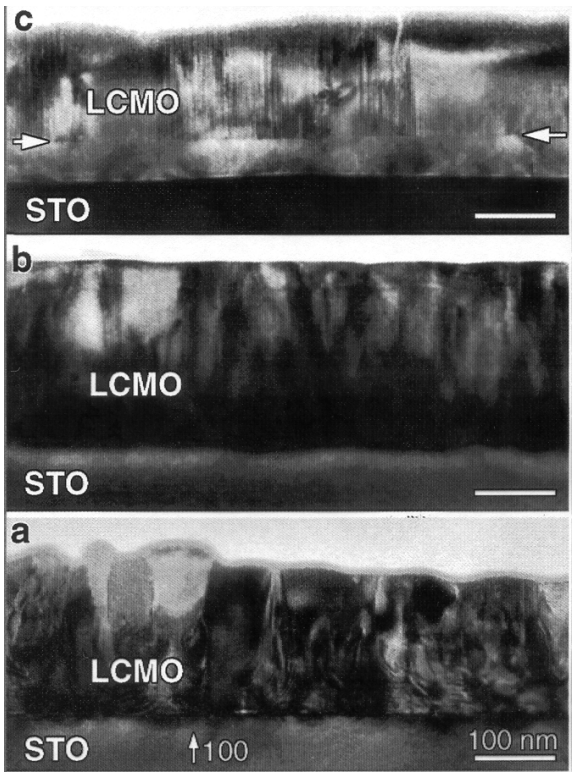

Figure 5. Low magnification multibeam bright-field diffraction contrast image of the columnar texture of $La_{0.7}Ca_{0.3}MnO_3$ films deposited at different substrate temperatures: (a) 530 °C, (b) 720 °C, (c) 890 °C. The substrate is STO terminated with a TiO_2 plane. Note that in (c) a perfectly epitaxial transition layer has been formed (white arrows) [22].

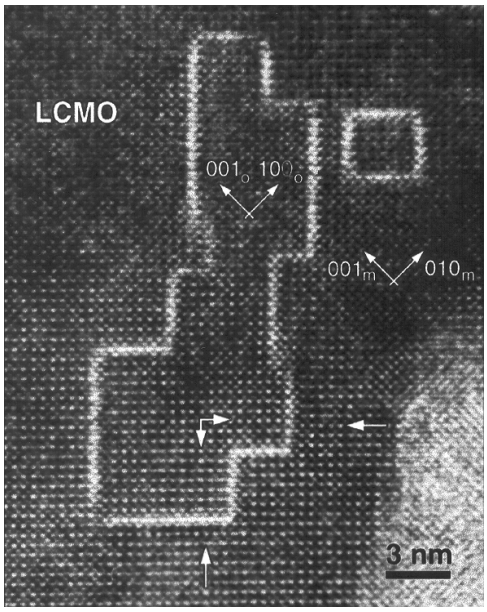

Figure 6. Plan-view HRTEM image along $[010]_o$ of a $La_{0.7}Ca_{0.3}MnO_3$ film deposited at 890 °C. Note the presence of polygonal islands within the pattern is in an antiphase relationship with respect to that in the surrounding matrix [22].

structure. However, taking into account the crystallographic data for bulk material, with composition $x = 0.3$, the x-ray diffraction pattern of films is indexed on an orthorhombic lattice with parameters $a \sim c = 0.5451$ nm ($a_p \approx a_p\sqrt{2}$) and $b = 0.7678$ nm ($\approx 2a_p$) resulting in a tensile strain with the STO substrate of 1.7%. Strain-induced microstructural changes are usually too small to lead to observable splitting of x-ray reflections. In this respect transmission electron microscopy (TEM) and, in particular, high-resolution electron microscopy may be the probes of choice. Distortions from original bulk symmetry can be investigated systematically. In an early study Lebedev *et al* [22] explored the evolution of the microstructure as a function of deposition temperature and film thickness. At low substrate temperature ($T_S = 530$ °C) the film has a grainy microstructure with an average grain size of about 40–100 nm. The contact plane between film and substrate is rough. At higher temperatures ~720 °C the grain size is larger and the film acquires a domain structure consisting of columns, elongated along the substrate normal, and separated by internal interfaces. The contact surface between film and interface becomes smoother, and dark areas, revealing faults and strains, are no longer visible. At the highest temperature ($T_S = 890$ °C) the film/substrate interface becomes flat and sharp and a perfectly monocrystalline layer with a thickness of about 100 nm, separating the substrate from the columnar structure, is formed. In figure 5 the low magnification multibeam bright field diffraction contrast images of $La_{0.7}Ca_{0.3}MnO_3$ films deposited at 530 °C (a), 720 °C (b) and 890 °C (c) are represented. In plan-view specimens the columns are visible as small domains surrounded by bright lines, which are identified as images of antiphase boundaries (figure 6). It is logical to assume that the closed polygonal antiphase boundaries in plan-view specimens, such as figure 6, are in fact cross sections of the columnar grains revealed in cross-section specimens. This interpretation is suggested by the good correlation between the average width of the columns in cross section and the average diameter of such polygons in plan view. Without elaborating the details buried in the TEM investigation the formation of monoclinic and orthorhombic phases at a certain distance away from the substrate/film interface is a different way for relaxation of substrate-induced strain. Up to a critical thickness, epitaxial films usually grow coherently strained. Thicker films may have a two-layer structure of a coherently strained bottom layer and a (partially) strain-relaxed, possibly defect-rich upper layer, both separated by a defect-rich interface.

4. Possibilities for extrinsic continuous tuning of intrinsic electronic inhomogeneities

The results given in sections 2 and 3 clearly show that fine tuning of deposition parameters and growth conditions can sensitively alter the microstructure of COTFs and thus their physical properties. To use the full potential of COTFs for applications, however, a continuous tuning of their properties is required. For extrinsic manipulation several possibilities exist, albeit not explored to a great extent. In this section some of them are briefly outlined.

4.1. Dynamical strain in epitaxially grown complex oxide thin films

A rather obvious way to externally manipulate macroscopic properties (resistivity, magnetization) in COTFs grown epitaxially is the use of piezoelectric substrates which allow a continuous variation of the strain state of the film by applying a voltage on the piezoelectric substrate. Zheng *et al* [23] have deposited $La_{0.7}Sr_{0.3}MnO_3$ thin films on piezoelectric $(1-x)Pb(Mg_{1/3}Nb_{2/3})O_3 - xPbTiO_3$ (PMN-PT) ($x \sim 0.3$) single-crystal substrates and studied the effects of substrate-induced lattice strain on the resistance of the LSMO films. By applying electric fields across the PMN-PT substrate, an in-plane compressive (tensile) strain in the PMN-PT substrate is induced *in situ* via the converse piezoelectric effect. The induced strain is transferred to the LSMO film, causing a linear decrease (increase) in the resistance of the LSMO film. A relationship between the resistance change $\Delta R/R$ and the strain ε_{zz} in the LSMO film is derived, indicating that the relative change in the resistance is proportional to the induced strain in the LSMO film. Compared with the strain state of the LSMO film when $E = 0$ kV mm^{-1}, the PMN-PT substrate imposes an in-plane compressive strain on the LSMO film when a positive electric field is applied to the positively polarized PMN-PT substrate. It was observed that the relative change in the resistance is proportional to the induced in-plane compressive strain in the LSMO film. Applying an electric field of 1 kV mm^{-1} to the PMN-PT substrate resulted in $\Delta R/R = 5.5\%$ and $\varepsilon_{xx} = 0.088\%$. Thus a resistance–strain coefficient $\Delta R/R/\varepsilon_{xx} = 67.1$ is obtained. In a similar experiment Thiele *et al* [24] used rhombohedral piezoelectric $Pb(Mg_{1/3}Nb_{2/3})_{0.72}Ti_{0.28}O_3(001)$ substrates and applied an electric field $E \leqslant 12$ kV cm^{-1}. The magnitude of the total variable in-plane strain has been derived and strain-induced shifts of the ferromagnetic Curie temperature T_c of up to 19 K were found in $La_{0.7}Sr_{0.3}MnO_3$ and $La_{0.7}Ca_{0.3}MnO_3$ films. These experiments demonstrate the possibility of electrical control of the metal–insulator transition temperature and T_C at practically relevant temperatures.

4.2. Photon-induced manipulation of manganite thin film properties

Exposing manganites to an x-ray photon flux novel interactions occur well beyond the conventional photoeffect. An interesting memory effect has been observed by Casa *et al* [25] when $La_{1-x}Sr_xMnO_3$ ($x \sim 1/8$) thin films are repeatedly exposed to x-rays. While the 'dark' conductivity remains unaffected by the irradiation history, the conductivity is markedly enhanced upon exposure to x-rays at low temperatures. In figure 7 a typical result is given showing that the electrical resistance at $T = 55$ K decays with cumulative dose in a manner similar to other manganites, following a stretched exponential time dependence. However, unlike $Pr_{1-x}Ca_xMnO_3$ and related compounds whose x-ray photoconductivity is persistent, in the $La_{0.88}Sr_{0.1}MnO_3$ film the resistance recovers to the dark level when the x-rays are switched off. When the material is again exposed to x-rays, the resistance falls very quickly to the *same* level attained immediately before the x-rays were switched off and resumes its decay with the same—much slower—time constant. Remarkably, the system thus retains a 'memory' of its history of past illuminations that is hidden when the x-ray beam is off. These findings are qualitatively explained by a model based on the interplay of three distinct and partially coexisting states: an orbitally ordered state observed before, a state with quenched orbital disorder, and a nonequilibrium state in which x-ray illumination helps to maintain orbital fluctuations and sustain an enhanced conductivity. The memory, which is encoded in the volume fraction of these phases, is an unexpected consequence of the phase separation.

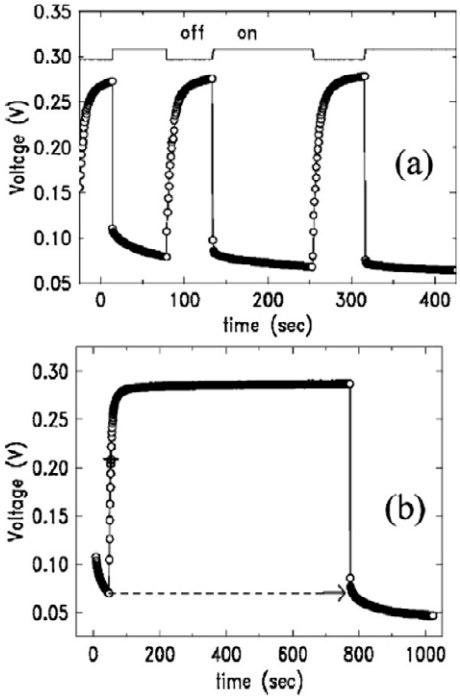

Figure 7. (a) Voltage at a constant current of 10 mA at $T = 55$ K monitored as a function of x-ray irradiation. The line above is the state of the x-ray shutter as indicated. (b) Detailed demonstration of the 'memory effect', showing that the memory is maintained for ~100 times the apparent recovery time constant (~7 s, taken as 63% of the rise). The x-rays are off during the time period indicated by the dotted line (~730 s). Note the very fast (<1 s) recovery of the original relaxation curve after the x-rays are switched on.

The list of possibilities to externally manipulate COTF properties can be extended to methods based on manipulating intrinsic anisotropy of the electronic system and their effects on thermoelectric properties of films. Zhang *et al* observed in-plane thermoelectric voltages in manganite thin films deposited on vicinal cut substrates and argued that the results are due to off-diagonal elements of the Seebeck tensor which in turn is a consequence of mesoscopic phase separation [26]. Albrecht *et al* investigated the magnetic interaction of the flux-line lattice and the magnetic domain structure in YBCO/LCMO heterostructures and observed intriguing possibilities to manipulate magnetically the properties of both the superconductor and the ferromagnet [27].

5. Conclusions

Complex oxide thin film and superlattice research is meanwhile based on a mature, albeit complex technology. Dedicated thin film research exploring details of complex oxide thin film growth develops a solid basis for a reliable thin film technology for these materials as the cornerstone for further research. Accomplishing the goal of mastering the technological prerequisites forms the basis to address the more materials physics oriented explorative research activities. Investigating fundamentals of interfacial strain generation and strain accommodation paves the way to intentionally manipulate thin film properties externally. Here, reversible biaxial dynamic strain, photon-induced modifications of phase separation, defect tailoring for flux-line and magnetic domain pinning is currently at the core. Finally, most recently the exploration of interface properties in complex oxide heterostructures and superlattices and the attempt to construct novel quantum states at the interface represent one of the most fascinating research areas in current thin film physics.

References

[1] Dagotto E 2002 *Nanoscale Phase Separation and Colossal Magnetoresistance* (Berlin: Springer)
[2] Esaki L and Tsu R 1969 *IBM J. Res. Dev.* **14** 61
[3] Grünberg P and Miko K 1983 *Phys. Rev.* B **27** 2955
[4] Ohtomo A and Hwang H Y 2004 *Nature* **247** 427
[5] Reyren N, Thiel S, Caviglia A D, Kourkoutis L F, Hammerl G, Richter C, Schneider C W, Kopp T, Ruetschi A S, Jaccard D, Gabay M, Muller D A, Triscone J M and Mannhart J 2007 *Science* **317** 1196
[6] Chakhalian J, Freeland J W, Srajer G, Strempfer J, Khaliullin G, Cezar J C, Charlton T, Dagliesh R, Bernhard C, Cristiani G, Habermeier H-U and Keimer B 2006 *Nat. Phys.* **2** 244
[7] Kennedy D (ed) 2007 *Science* **317** 1844
[8] Borrmann R and Nölting J 1989 *Appl. Phys. Lett.* **54** 2148
[9] Venderah T A 1991 *Chemistry of Superconducting Oxides* (New York: Noyes)
[10] Raistrick I D *et al* 1993 *Interfaces in High T_c Superconducting Systems* ed S L Shinde and A Rudman (Berlin: Springer) p 28
[11] Somekh R E *et al* 1992 *Concise Encyclopedia of Magnetic and Superconducting Materials* ed J Evetts (Oxford: Pergamon) p 431
[12] Naito M, Yamamoto H and Sato H 1998 *Physica* C **305** 233
[13] Habermeier H-U 2004 *J. Electroceram.* **13** 23
[14] Kawasaki M, Takahashi K, Maeda T, Tsuchiya R, Shinohara M, Ishiyama O, Yonezawa T, Yoshimoto M and Koinuma H 1994 *Science* **266** 1540
[15] Koster G, Kropman B L, Rijnders G J H M, Blank D H A and Rogalla H 1998 *Appl. Phys. Lett.* **73** 2920
[16] Haage T, Haage T, Zegenhagen J, Li J Q, Habermeier H-U and Cardona M 1997 *Phys. Rev.* B **56** 8404
[17] Wang Z-H, Cristini G and Habermeier H-U 2003 *Appl. Phys. Lett.* **82** 3731
[18] Habermeier H-U 2007 *Mater. Today* **10** 34
[19] Lebedev O I and van Tendeloo G 2004 *Z. Metallk.* **95** 4
[20] Razavi F S, Gross G, Habermeier H-U, Lebedev O I, Amelinckx S, Van Tendeloo G and Vigliante A 200 *Appl. Phys. Lett.* **76** 175
[21] Lebedev O I, Van Tendeloo G, Amelinckx S, Razavi F S and Habermeier H-U 2001 *Phil. Mag.* A **81** 797
[22] Lebedev O I, Van Tendeloo G, Amelinckx S, Leibold B and Habermeier H-U 1998 *Phys. Rev.* B **58** 8065
[23] Zheng R K, Wang Y, Chan H L W, Choy C L and Luo H S 2007 *Phys. Rev.* B **75** 212102
[24] Thiele C, Dörr K, Bilani O, Rödel J and Schultz L 2007 *Phys. Rev.* B **75** 054408
[25] Casa D, Keimer B, Zimmermann M v, Hill J P, Habermeier H-U and Razavi F S 2001 *Phys. Rev.* B **64** 100404(R)
[26] Zhang P X and Habermeier H-U 2008 *J. Nanomater.* at press
[27] Albrecht J, Djupmyr M, Soltan S, Habermeier H-U, Connolly M and Bending S 2007 *New J. Phys.* **9** 1